Dalton Transactions

ROYAL SOCIETY OF CHEMISTRY

PAPER

View Article Online
View Journal | View Issue

Published on 23 September 2020. Downloaded by University of Rochester on 10/20/2020 11:52:45 AM.

Check for updates

Cite this: *Dalton Trans.*, 2020, **49**, 13737

Received 20th August 2020,
Accepted 21st September 2020

DOI: 10.1039/d0dt02931a

rsc.li/dalton

# Conducting neutral gold bisdithiolene complex $[Au(dspdt)_2]^{\bullet}$†

Mariana F. G. Velho,[a,b] Rafaela A. L. Silva,[a] Graça Brotas,[a] Elsa B. Lopes, [a,c] Isabel C. Santos, [a,c] Ana Charas,[b] Dulce Belo [*a,c] and Manuel Almeida [*a,c]

$[Au(dspdt)_2]$ (dspdt = 2,3-dihydro-5,6-selenophenedithiolate) is an unprecedented example of a neutral gold bisdithiolene complex with a unique structure composed of interacting dimer and trimer chains displaying relatively high electrical conductivity (0.1 S $cm^{-1}$ at room temperature).

## Introduction

Considering very significant developments in the field of molecular conducting materials during the last decades several hundred molecular metals and superconductors are presently known.[1] The large majority of molecular conductors are compounds based on two components, such as charge transfer salts, in which at least one electron donor or acceptor molecule becomes partially oxidised and builds in the solid an extended network of interactions, leading to partially filled bands responsible for electrical conducting properties. In contrast, the possibility to achieve metallic properties in molecular solids based on a single component, as in elemental metals, is a much less explored possibility.[2–5]

The difficulty in obtaining molecular metals based on single components arises from the fact that the large majority of stable molecules are characterised by a large HOMO–LUMO gap and these frontier orbitals led, in the solid state, to valence and conductions bands, respectively, separated by large energy gaps. In this context, radical species were since early pointed out as good candidates, since the unpaired electrons could lead to partially filled bands without the need of charge transfer to or from any other molecular unit.[6] However, in spite of several attempts using delocalised planar radicals based on phenalenyl-[7,8] and thiazolyl-based radicals,[9–11] coupled TTFs (TTF = tetrathiafulvalene) and radical units,[12] or neutral gold bisdithiolene complexes[13–15] this possibility has been largely unsuccessful. Almost all such solids behave as insulators or poor semiconductors, except in a few cases if under high pressure.[11,16,17] This failure arises because the typical intermolecular interactions are relatively weak and lead to electron bandwidths significantly smaller than the on-site electron repulsion interactions. Therefore, half-filled bands generated from singly occupied states (SOMO bands) in molecular solids behave invariably as Mott-insulators.

The first well-succeeded examples of single component molecular solids with metallic properties at ambient pressure have been provided by molecules with small HOMO–LUMO gaps and large intermolecular interactions. These conditions allow the overlap between the valence and conduction bands, which become partially filled as in a semimetal. This possibility was early suggested for $[M(dmit)_2]$ (M: Ni, Pd, dmit = 4,5-dimercapto-1,3-dithiole-2-thione) complexes,[18] and later found in the first single component molecular metal characterised as a single crystal, a neutral nickel bisdithiolene complex $[Ni(tmdt)_2]$, (tmdt = trimethylenetetrathiafulvalenedithiolate), based on an highly extended dithiolene ligand fused with a TTF moiety.[3] Metallic behaviour has also been observed in neutral bisdithiolene complexes of nickel and other metals based on similar type of ligands with TTF moieties.[4] Although this type of extended ligands are regarded as good candidates, as they have low-HOMO–LUMO gaps and can promote large intermolecular interactions, highly conducting properties have also been observed at ambient pressure in a few gold complexes with smaller ligands,[2,5] in other purely organic molecular units such as catechol functionalised[19] or zwiterionic TTF derivatives.[20] A stable and highly conducting metallic state was recently achieved at ambient pressure in a neutral gold bisdithiolene complex with a thiazoldithiolate ligand, as a consequence of a larger superposition of SOMO and SOMO−1 bands, with electron transfer from the last to the first one.[5]

Here we report a selenium derivative of $[Au(\alpha\text{-tpdt})_2]$ (α-tpdt = 2,3-thiophenedithiolate),[2] $[Au(dspdt)_2]$ (dspdt = 2,3-

[a]*Centro de Ciências e Tecnologias Nucleares, Instituto Superior Técnico, Universidade de Lisboa, E.N. 10, P-2695-066 Bobadela LRS, Portugal. E-mail: dbelo@ctn.tecnico.ulisboa.pt, malmeida@ctn.tecnico.ulisboa.pt*
[b]*Instituto de Telecomunicações, Instituto Superior Técnico, Av. Rovisco Pais 1, P-1049-001 Lisboa, Portugal*
[c]*Departamento de Engenharia e Ciências Nucleares, Instituto Superior Técnico, Universidade de Lisboa, E.N. 10, P-2695-066 Bobadela LRS, Portugal*

†Electronic supplementary information (ESI) available: Fig. S1–S8 and Tables S1–S9. CCDC 2015926–2015928. For ESI and crystallographic data in CIF or other electronic format see DOI: 10.1039/d0dt02931a

Published on 23 September 2020. Downloaded by University of Rochester on 10/20/2020 11:52:45 AM.

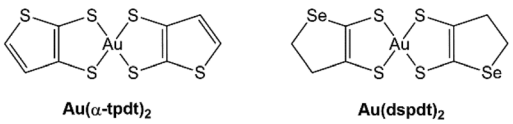


**Chart 1** Chemical structures of gold bisdithiolene complexes with thiophene and selenacyclopentane, respectively.

dihydro-5,6-selenophenedithiolate) (Chart 1). This new derivative displays an unusual structural arrangement composed of a combination of interacting dimer and trimer columns and semiconducting properties with relatively high electrical conductivity associated with the splitting of closely spaced energy bands derived from SOMOs.

## Results and discussion

The key compound to prepare [Au(dspdt)$_2$] is thione **1** (5,6-dihydroselenolo[2,3-*d*]-1,3-dithiole-2-thione), obtained by a modified version of a previously described procedure (Scheme 1).[21] The synthesis of **1** is based on a previously reported procedure by Jigami *et al.*,[21] however with some modifications since for us the method described to obtain the first intermediate (**A**) was not reproducible. The synthesis of this compound starts with a cyclization reaction of commercial available 2-(3-butynyloxy)tetrahydro-2*H*-pyran with *n*BuLi, sulphur and carbon disulphide, giving the 1,3-dithiole-2-thione ring. This reaction was performed without the reported addition of tetramethylethylenediamine or MeOH.[21] Afterwards, selenium powder was added and the reaction was quenched with MeI, giving **A**.

Selected single crystals enabled the determination of the crystal structure of **1** by X-ray diffraction (Tables S1, S2 and Fig. S1, S2†). The molecule is planar, with exception of the ring ethyl groups (Fig. S1†). The crystal structure of **1** is composed by head-to-tail columns, running along *a* (Fig. S2b†). Along the columns the molecules are connected by C–H···S hydrogen bonds. Between columns, neighbouring molecules are connected through an intricate 3D network of S···S and S···Se short contacts (Fig. S2a/c†).

The monoanionic gold complex, *n*Bu$_4$N[Au(dspdt)$_2$] **2**, was prepared following a general procedure, commonly used to prepare similar bisdithiolene complexes (Scheme 1).[2] The ligands were obtained in solution from **1** by an hydrolytic cleavage with sodium methoxide in methanol, followed by addition of potassium tetrachloroaurate(III), leading to the precipitation of the corresponding tetrabutylammonium (**2a**) or tetraphenylphosphonium (**2b**) salts after treatment with *n*Bu$_4$NBr or Ph$_4$PBr, respectively. The tetraphenylphosphonium salt is easier to prepare and has a more reasonable yield than **2a**, which could only be obtained as a few dark brown needle shaped crystals suitable for X-ray diffraction, demonstrating the formation of the anionic complex (Tables S3–S6 and Fig. S3, S4†).

In the crystal structure of **2a**, the anionic complex presents a square planar coordination geometry (Fig. 1) with S–Au distances of 2.32 Å and a small boat distortion due to hydrogen bonds between the cations involving sulphur and selenium atoms. The selenium atoms appear disordered over two equi-populated positions denoting either *cis–trans* disorder or most likely an orientation disorder of *trans* configuration. The crystal structure is composed by consecutive anionic grid layers, growing in the *bc* plane. Apart a few intermittent Se···Se short contacts between anions, the molecules in the layers are separated at distances slightly above the sum of the van der Waals radii. There is no interactions between anions in neighbouring layers. The cations occupy the empty space in this honeycomb anionic structure, contacting with the anions throughout several S···H–C hydrogen. Further details are given in Tables S3–S6 and Fig. S3, S4.†

The redox properties of **2**, studied by cyclic voltammetry, show a pair of redox waves centred at $E_{1/2}$, of 42.5 mV *vs.* Ag/AgNO$_3$ ($E_{1/2}$(Fc/Fc$^+$) = 357 mV), (Fig. 4) ascribed to the couple [Au(dspdt)$_2$]$^-$/[Au(dspdt)$_2$]$^0$ indicating the possibility to obtain the neutral complex **3** as a stable compound.

Indeed, the oxidation of the monoanionic complex **2** to give the neutral complex **3** could be carried out with iodine in solu-

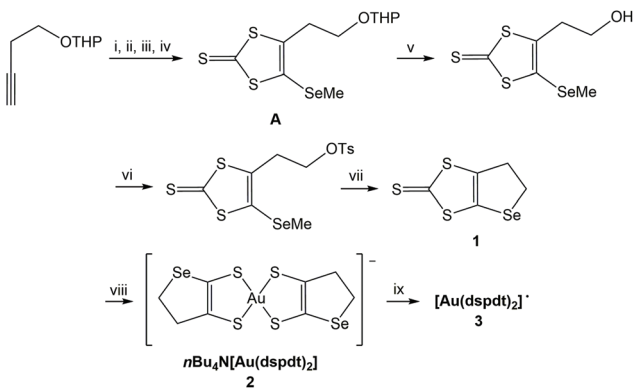


**Scheme 1** Synthesis of the thione **1** and monoanionic (**2**) and neutral (**3**) gold complexes [Au(dspdt)$_2$]: (i) *n*BuLi, THF, −78 °C; (ii) S, 0° C; (iii) CS$_2$, −78° C; (iv) Se then MeI, 0° C; (v) HCl (aq.), acetone/MeOH; (vi) TsCl, pyridine; (vii) NaI, DMF, 80 °C; (viii) DDQ, toluene, reflux. (viii) MeONa, KAuCl$_4$ in MeOH, *n*Bu$_4$NBr (**2a**) or Ph$_4$PBr (**2b**) in MeOH; (ix) treatment with an iodine solution in acetone or electrochemical oxidation at constant potential.

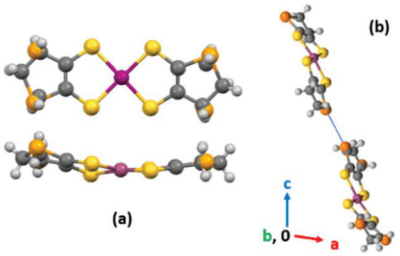


**Fig. 1** (a) Top and side view of the [Au(dspdt)$_2$]$^-$ complex in **2a**, (b) short contacts between anion pairs in plane *b*, *c*.


This journal is © The Royal Society of Chemistry 2020

Published on 23 September 2020. Downloaded by University of Rochester on 10/20/2020 11:52:45 AM.

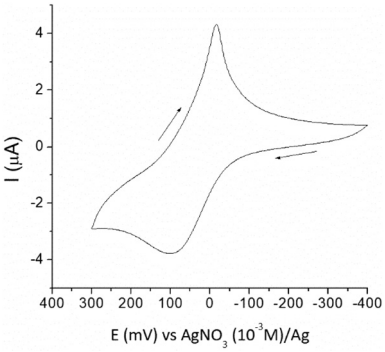


**Fig. 2** Cyclic voltammetry of $[Au(dspdt)_2]^-$ in $CH_2Cl_2$, 0.5 × $10^{-3}$ M with $nBu_4NPF_6$ 0.1 M as supporting electrolyte, *E* [V] *vs.* $Ag/AgNO_3$, Pt electrode and scan rate 100 mV $s^{-1}$. The ferrocene/ferrocenium ($Fc/Fc^+$) couple was measured in the same conditions, displaying a $E_{1/2}$ = 357 mV *vs.* $Ag/AgNO_3$.

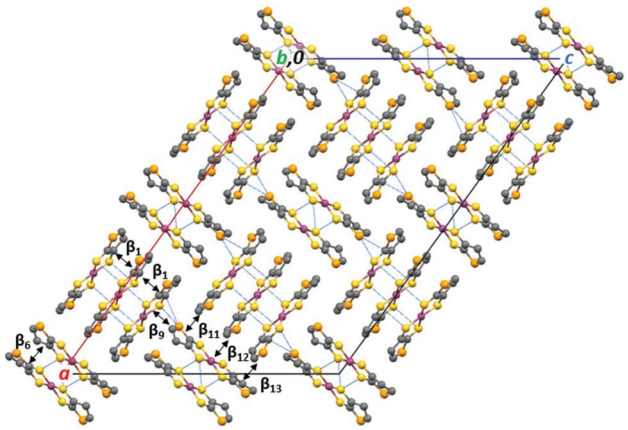


**Fig. 3** Crystal structure of **3**, $[Au(dspdt)_2]^{\bullet}$, viewed along *b* axis. Only one *trans* configuration for the disordered Se atoms was considered. The thin blue lines denote short contacts.

tion, giving a dark fine powder. As an alternative, the oxidation can be done electrochemically at a constant potential (300 mV *vs.* $Ag/AgNO_3$) yielding small dark needle crystals (up to 0.5 × 0.03 × 0.03 $mm^3$) suitable for X-ray diffraction.

The asymmetric unit of **3** contains two neutral complex units A and B in general position and half complex C with the gold atom in an inversion center (Fig. S5†). As often observed in similar thiophenic complexes the Se atoms appear disordered between two positions, most likely resulting from the usual orientation disorder of *trans* configuration.[22,23] With exception of a small distortion in the ethylene groups the complexes are essentially planar with unit B presenting a small boat type distortion. The Au–S bond lengths (~2.31 Å) are comparable to other neutral gold bisdithiolene complexes (Tables S7 and S8†). A comparative analysis between the bond lengths in the neutral and monoanionic gold complexes shows a shortening of the $S_{coord}$–C bond length (1.75 Å in **2** and 1.69 Å in **3**), while the Au–S remains essentially the same, denoting a ligand centered oxidation process.[23]

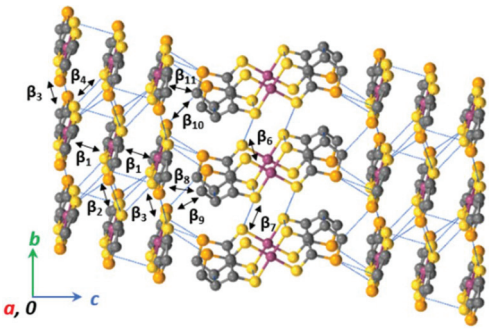


**Fig. 4** Nearby dimer and trimer columns in **3** viewed along *a* axis.

The neutral complexes are arranged as centrosymmetric A–A dimers and B–C–B trimers, where the molecules overlap parallel to each other with a metal-over-metal mode with short interplane distances of 3.581 Å and 3.622 Å respectively, and with several intermolecular atomic distances well below the sum of van der Waals radii (Table S9†).

The unit cell contains 20 neutral complex units organised in four trimers and four dimers, as shown in Fig. 3. The crystal structure is composed of columns along *b* of closely spaced side-by-side dimers and columns of trimers (Fig. 2 and Fig. S6†). The dimer and trimer columns alternate in the *a*,*c* plane in such a way that each trimer column is surrounded by 4 next neighbour dimer columns and each dimer column is surrounded by 4 columns of trimers. The arrangement in dimers is quite common in neutral gold bisdithiolene complexes,[13,14] as well as in other radical species, driven by the strong pairing interaction of SOMOs. However, the formation of trimers is quite uncommon and the present structural type composed of a mixture of dimer and trimer columns is to the best of our knowledge unprecedented.

Electrical conductivity was measured in small single crystals and showed a value of 0.1 S $cm^{-1}$ at room temperature, following a semiconducting behaviour with an activation energy of 95 meV (Fig. 5). This conductivity, although not as large as other single component compounds behaving as metals at ambient pressure, such as $[Au(\alpha\text{-}tpdt)_2]$ (7 S $cm^{-1}$ in polycrystalline sample),[2] $[Au(tmdt)_2]$ (50 S $cm^{-1}$ in crystalline

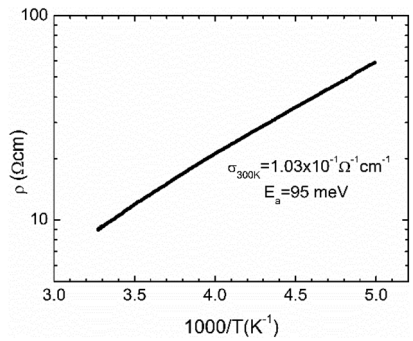


**Fig. 5** Temperature dependence of electrical resistivity, $\rho$, of $[Au(dspdt)_2]^{\bullet}$.

Published on 23 September 2020. Downloaded by University of Rochester on 10/20/2020 11:52:45 AM.

sample)[24] and [Au(Me-thiazdt)$_2$] (Me-thiazdt = *N*-methyl-1,3-thiazoline-2-thione-4,5-dithiolate, 750 S cm$^{-1}$ in single crystals),[5] is rather large for a single-component material based on a gold complex.[25–27]

The electrical properties of this compound can be understood in view of the intermolecular electronic interactions and the resulting electronic band structure. With 20 molecules in the unit cell, each with different possible configurations of Se atoms, the number of different intermolecular interactions is rather large. Their magnitude is expected to be quite different, depending on the type of contacts, and can be estimated using an extended Hückel approach.[28–31] For sake of simplicity in the analysis of the different intramolecular interactions, only one *trans* configuration was considered.

As seen in Table 1 the largest $|\beta_{HOMO-HOMO}|$ energy interactions are between closely spaced face-to-face molecules in the trimer ($\beta_1$ = 907 meV) and dimer ($\beta_6$ = 998 meV). Along *b* the trimers are arranged in columns with side-by-side interactions $\beta_2$, $\beta_3$ and $\beta_4$, with values of 114, 100 and 28 meV, respectively. The dimers along the columns present also side-by-side interactions of smaller magnitude, $\beta_5$ = 17 and $\beta_7$ = 36 meV. In addition, there are intercolumn interactions $\beta_7$–$\beta_{13}$, with values listed in Table 1. The intercolumn interactions are quite anisotropic being more significant along the long axis of the dimers reaching 100 meV for $\beta_8$, while they are significantly smaller along *a*.

Based on the intermolecular interactions it is possible to estimate the electronic band structure using a tight-binding extended Hückel approach.[28–31] The 20 donor molecules in the unit cell lead to 20 bands derived from the SOMO orbital around the Fermi level, as shown in Fig. 6 (additional band structures and Fermi surface in Fig. S7 and S8†). These bands result from a combination of mixed trimer and dimer parallel bands that due to intercolumn interactions are considerably split and partially overlapping. The two upper sets of 4 bands result from an avoided crossing between the upper trimer and the dimer SOMO bands, with larger and smaller dispersions, respectively. The Fermi level crosses the central four bands, mostly due to the nonbonding SOMO combination of the trimers. The Fermi level is very close to the top of a lower set of four bands along Γ–X, derived mainly from the lower dimer orbitals.

This band structure can be understood recalling that a single chain of strong radical dimers has two SOMO bands, the lower one full and the upper one empty. On the other end a single chain of trimers will lead to three SOMO bands, the middle one half filled. Therefore, the chains of radical dimers are expected to lead to semiconducting properties due to the large dimer gap, while the trimer chains will behave as Mott insulators, as observed in all molecular materials with half-filled bands due to on-site electron–electron repulsion interactions larger than the bandwidth. The above situation, expected for isolated chains, contrasts with the present case where, due to the significant intercolumn interactions between dimers and trimer chains, there is a strong splitting of the bands in sets of 4, with the Fermi level crossing the four central bands at different wave vectors.

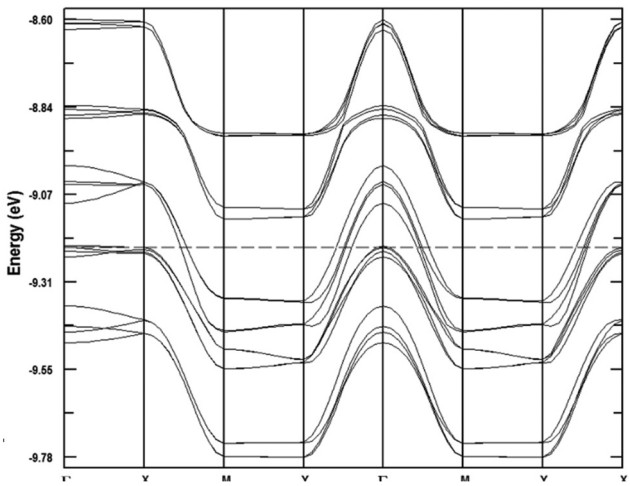


Fig. 6 Calculated band structure of [Au(dspdt)$_2$]$^{\bullet}$, 20 SOMO bands near the Fermi level (dashed line). The. Γ, X, Y and M and refer to the (0, 0, 0), ($\frac{1}{2}$, 0, 0), (0, $\frac{1}{2}$, 0), ($\frac{1}{2}$, $\frac{1}{2}$, 0), points in *k*-space, respectively.

Table 1 $\beta_{HOMO-HOMO}$ energy interactions represented in Fig. 3 and Fig. 2, in eV

| $\beta$ (eV) | | | | | | |
|---|---|---|---|---|---|---|
| $\beta_1$ | $\beta_2$ | $\beta_3$ | $\beta_4$ | $\beta_5$ | $\beta_6$ | $\beta_7$ |
| 0.907 | 0.114 | 0.100 | 0.028 | 0.017 | 0.998 | 0.036 |
| $\beta_8$ | $\beta_9$ | $\beta_{10}$ | $\beta_{11}$ | $\beta_{12}$ | $\beta_{13}$ | $\beta_{14}$ |
| 0.103 | 0.006 | 0.010 | 0.011 | 0.004 | 0.027 | 0.041 |

Although **3** is highly conducting for a solid composed of a single neutral species, it is not metallic as predicted by this ideal model without electron correlation effects, but rather semiconducting with relatively high conductivity and low activation energy. Although the Fermi level lies close to the lower set of dimer bands, the compound is still in the range of Mott-insulator with unpaired electrons localized in each trimer. In addition, the disorder in the Se atoms position, not taken into account in the calculations, where only one *trans* configuration for the complexes was assumed, may also contribute to the electronic localisation.

# Experimental

### General information

All reactions were carried out under a nitrogen atmosphere with dry solvents, unless otherwise stated. All solvents were dried and distilled following the standard procedures.[32] All the reagents used on the synthesis, including the starting material 2-(3-butynyloxy)tetrahydro-2*H*-pyran, were purchased from commercial sources and used without any additional purification.

 This journal is © The Royal Society of Chemistry 2020

Published on 23 September 2020. Downloaded by University of Rochester on 10/20/2020 11:52:45 AM.

**Synthesis of 4-Methylseleno-5-[2-(tetrahydropyran-2-yloxy) ethyl]-1,3-dithiole (A).** Modified procedure based on the one described by Jigami *et al.*:[21] To a solution of 2-(3-butynyloxy) tetrahydro-2*H*-pyran (1.26 mL, 7.80 mmol) in THF (47 mL) was added a solution of *n*BuLi in hexane (1.6 M, 5.0 mL) at −78° C and the mixture was stirred for 30 min at the same temperature. Then sulphur (250 mg, 7.80 mmol) was added and the mixture was allowed to slowly warmed to 0° C over a period of 2 h and stirred at this temperature for other 2 h. Carbon disulphide (0.5 mL, 7.80 mmol) and selenium (616 mg, 7.80 mmol) were added at −78 °C and the mixture was again warmed to 0° C over a period of 2 h and then stirred at the same temperature for another hour. The reaction was quenched with methyl iodide (0.5 mL, 7.80 mmol) and after stirring 1 h at 0° C, water (12 mL) was added to the mixture. The mixture was extracted with $CH_2Cl_2$, washed with brine and dried with $MgSO_4$. The product was purified by column chromatography on silica gel with $CH_2Cl_2$, giving 1.46 g of **A** as a yellow oil. Yield 52%. $^1$H NMR (300 MHz, $CDCl_3$): $\delta$ 4.60 (br tr, $J$ = 3.04, 1H), 3.89 (m, 1H), 3.76 (m, 1H), 3.50 (m, 2H), 3.06 (m, 2H), 2.30 (s, 3H), 1.5–1.9 (m, 6H).

**Synthesis of [*n*Bu$_4$N][Au(dspdt)$_2$] (2a).** Compound **1** (100 mg, 0.42 mmol) was added to a solution of sodium methoxide in methanol, obtained by a complete reaction of metallic sodium (46 mg, 2 mmol) in methanol (10 mL). After stirred at 40 °C for 45 min, a solution of potassium tetrachloroaurate (79.3 mg, 0.21 mmol) in methanol (1 mL) was added and the mixture was stirred for an extra 1 h. The mixture was filter into a solution of tetrabutylammonium bromide (67.7 mg, 0.21 mmol) in methanol (5 mL). There was no visible formation of precipitate. The golden-brown solution was then cooled and kept under a low flux of nitrogen. Maintaining these conditions during several days was possible to collect dark brown crystals suitable for single crystals X-ray studies. FTIR (KBr), cm$^{-1}$: 685 (w, C–S), 736 (s, C–H aliph), 875 (m, C–H aliph), 1241 (s, $H_2C$–$CH_2$ ligand), 1380 (m, C–H aliph), 1458 (m, C–H aliph), 1632 (m, C═C), 2858 (m, C–H aliph), 2954 (m, C–H aliph). UV-Vis ($CHCl_3$): $\lambda_{max}$ = 370, 418 nm.

**Synthesis of [PPh$_4$][Au(dspdt)$_2$] (2b).** This compound was prepared following the same procedure as for **2a**, using tetraphenylphosphonium bromide (105.7 mg, 0.252 mmol) in methanol (1 mL), instead of tetrabutylammonium bromide. After standing for a few hours, the reaction mixture was filtered and the collected solid was washed with methanol and diethyl ether. Compound **2b** (96 mg) was obtained as a brownish powder. Yield 50%. Elemental analysis calcd (%) for $C_{32}H_{28}AuPS_4Se_2$: C 41.48, H 3.04, S 13.84; found C 40.53, H 2.99, S 13.11.

**Synthesis of [Au(dspdt)$_2$]$^\bullet$ (3). Procedure a**: To a solution of **2b** (30 mg, 0.032 mmol) in acetone (3 mL) was added a solution of iodine (9 mg, 0.036 mmol) in acetone (1 mL). The mixture was stirred for 15 min and the collected solid was washed with acetone, yielding 24.3 mg (86%) of **3** as black crystalline powder. Elemental analysis calcd (%) for $C_8H_8AuS_4Se_2$: C 16.36, H 1.37, S 21.84; found C 18.35, H <2.0, S 20.26. **Procedure b**: A dichloromethane solution containing **2a** (0.5 × $10^{-3}$ M) and tetrabutylammonium hexafluorophosphate (0.1 M) undergo an electrochemical oxidation process at a constant potential of 300 mV, during 4000 s. At the end, compound **3** was collected has small dark needles. FTIR (KBr), cm$^{-1}$: 1256 (s, $H_2C$-$CH_2$ ligand), 1358 (m, C–H aliph), 1637 (m, C═C).

### Cyclic voltammetry studies

Cyclic voltammetry data were obtained using a BAS C3 Cell Stand. The voltammograms were obtained at room temperature with variable scan rates in the range of 20–500 mV s$^{-1}$, platinum wire working and counter electrodes and a Ag/$AgNO_3$ (0.01 M $AgNO_3$ and 0.1 M *n*$Bu_4NPF_6$ in acetonitrile) reference electrode, in which the $Ag^+$ ion electrode was separated from the bulk solution by a Vycor™ frit. The measurements were performed on fresh solutions with a concentration of 0.5 × $10^{-3}$ M, in dichloromethane, that contained *n*$Bu_4NPF_6$ (0.1 M) as a supporting electrolyte. Ferrocene was added directly to the solution after analysis to allow the potentials normalization *in situ*, relatively to the ferrocene/ferrocenium couple redox potential. Under the experimental conditions the ferrocene/ferrocenium ($Fc/Fc^+$) couple was found to bet $E_{1/2}$ = 357 mV *vs.* Ag/$AgNO_3$.

### X-ray crystallography

Crystallographic and experimental details of data collection and crystal structure determinations for the compounds **1**, **2a** and **3** are given in Table 2. Suitable crystals of these compounds were mounted on a loop in Fomblin protective oil and data were collected on a Bruker APEX II area detector diffractometer at 150 K using graphite-monochromated Mo Kα ($\alpha$ = 0.71073 Å) in the φ and ω scans mode. Cell parameters were retrieved using Bruker SMART and refined using Bruker SAINT on all observed reflections.[33] Absorption corrections were applied using SADABS.[34] The structures were solved by direct methods using either SHELXS-97[35] or SIR 97[36] and refined using full-matrix least squares refinement against $F^2$ using SHELXL-2014.[37] In the former case, all programs are included in the package of programs WINGX-v2014.1.[38] All non-hydrogen atoms were refined anisotropically, unless it was mentioned in the cif files of the structures, and all hydrogen atoms were placed in idealized positions and allowed to refine riding on the parent carbon atom. Molecular graphics and packing diagrams were prepared using MERCURY-4.3.[39] (CCDC 2015926, 2015927 and 2015928† contain supplementary crystallographic data for **1**, **2a** and **3** respectively).

### Electric transport properties

Electrical conductivity measurements were made along the needle axis of the crystals in the temperature range of 200–310 K, using a measurement cell attached to the cold stage of a closed cycle helium refrigerator. A four-in-line contact standard configuration DC method was used to perform these measurements, using a Keithley 224 current source to apply through the sample both direct and reverse DC currents, and Keithley 619 electrometer to measure the corresponding voltage drop, the current used was 1 μA.

Published on 23 September 2020. Downloaded by University of Rochester on 10/20/2020 11:52:45 AM.

Table 2 Selected crystal data and data collection parameters for **1**, **2a** and **3**

| | **1** | **2a** | **3** |
|---|---|---|---|
| Empirical formula | $C_5H_4S_3Se_1$ | $C_{24}H_{44}N_1S_4Se_2Au$ | $C_{40}H_{40}S_{20}Se_{10}Au_5$ |
| Crystal size (mm) | 0.35 × 0.10 × 0.06 | 0.20 × 0.02 × 0.02 | 0.14 × 0.02 × 0.02 |
| Formula weight | 239.22 | 829.73 | 2936.35 |
| Cryst. system | Orthorhombic | Monoclinic | Monoclinic |
| Space group | *Pbca* | *P*21/*c* | *C*2/*c* |
| *a* [Å] | 7.4929(2) | 9.4015(3) | 40.7970(14) |
| *b*[Å] | 11.7270(3) | 17.8349(5) | 6.4600(2) |
| *c* [Å] | 16.9268(5) | 17.9831(5) | 29.1807(9) |
| *α* [°] | 90 | 90 | 90 |
| *β* [°] | 90 | 98.102(2) | 125.8850(10) |
| *γ* [°] | 90 | 90 | 90 |
| *V* [Å$^3$] | 1487.34(7) | 2985.22(15) | 6230.8(4) |
| *Z*, $D_{Cal}$ (mg m$^{-3}$) | 8, 2.137 | 4, 1.846 | 4, 3.130 |
| *μ* (mm$^{-1}$) | 5.791 | 7.661 | 18.278 |
| $T_{min}/T_{max}$ | 0.2364/0.7226 | 0.310/0.862 | 0.184/0.711 |
| *F* (000) | 928 | 1624 | 5340 |
| *θ* range (°) | 3.44–25.34 | 2.935–25.680 | 3.419–26.371 |
| Index range (*h*, *k*, *l*) | −5/9; −14/12; −20/20 | −9/11; −21/21; −21/21 | −50/50; −7/8; −36/36 |
| Refle. collected/unique ($R_{int}$) | 7754/1354 (0.0407) | 29 859/5637 (0.0654) | 24 508/6326 (0.0993) |
| Data/restraints/parameters | 1354/0/82 | 5637/22/313 | 6326/112/381 |
| Final *R* indices [$I > 2\sigma(I)$] | $R_1$ = 0.0184, w$R_2$ = 0.0449 | $R_1$ = 0.0343, w$R_2$ = 0.0586 | $R_1$ = 0.0522, w$R_2$ = 0.0804 |
| GOF on $F^2$ | 1.054 | 1.037 | 0.969 |
| Largest diff. peak, hole/e Å$^{-3}$ | 0.327, −0.278 | 1.425, −1.471 | 1.425, −1.471 |
| CCDC reference† | 2015926 | 2015927 | 2015928 |

### Intermolecular energy interactions and band structure calculations for 3

The electronic band structure and intermolecular energy interactions were calculated using the freeware PrimeColor Software, CAESAR,[28] which employs the extended Hückel method[29–31] with a basis set consisting of Slater type orbitals of double-ζ quality. The exponents, contraction coefficients, and atomic parameters were taken from previous reported work.[18]

## Conclusions

In conclusion, [Au(dspdt)$_2$] is a rare case of a conducting compound based only on a single neutral unit with a new structural type composed of dimers and trimers. At variance with other single-component molecular metals, where the metallic properties arise from the overlap of HOMO and LUMO or SOMO−1 and SOMO bands, the highly conducting properties of [Au(dspdt)$_2$] result from the splitting of several quasi-one-dimensional SOMO bands from dimers and trimers that become non-degenerate due to the multiple interactions between chains in the unit cell. For slightly larger intermolecular interactions, which can be induced by high pressure, truly metallic properties are expected to be easily achieved in this situation. Although a crystal structure determination was never possible in [Au(α-tpdt)$_2$], this new alternative mechanism to high conductivity may explain the conducting metallic properties observed in that compound and other neutral gold complexes with small ligands.

## Conflicts of interest

There are no conflicts to declare.

## Acknowledgements

This work was partially supported by FCT (Portugal) through Contracts UIDB/04349/2020, UIDB/50008/2020 and PTDC/QUI-QIN/29834/2017, PhD grant PD/BD/135314/2017 to M. F. G. V. Fruitful discussions with E. Canadell are also acknowledged.

## Notes and references

1 P. Batail, *Chem. Rev.*, 2004, **104**, 4887–4890.
2 D. Belo, H. Alves, E. B. Lopes, M. T. Duarte, V. Gama, R. T. Henriques, M. Almeida, A. Pérez-Benítez, C. Rovira and J. Veciana, *Chem. – Eur. J.*, 2001, **7**, 511–519.
3 H. Tanaka, Y. Okano, H. Kobayashi, W. Suzuki and A. Kobayashi, *Science*, 2001, **291**, 285–287.
4 A. Kobayashi, E. Fujiwara and H. Kobayashi, *Chem. Rev.*, 2004, **104**, 5243–5264.
5 Y. Le Gal, T. Roisnel, P. Auban-Senzier, N. Bellec, J. Íñiguez, E. Canadell and D. Lorcy, *J. Am. Chem. Soc.*, 2018, **140**, 6998–7004.
6 R. C. Haddon, *Nature*, 1975, **256**, 394–396.
7 S. K. Pal, M. E. Itkis, F. S. Tham, R. W. Reed, R. T. Oakley and R. C. Haddon, *Science*, 2005, **309**, 281–284.
8 S. K. Pal, P. Bag, M. E. Itkis, F. S. Tham and R. C. Haddon, *J. Am. Chem. Soc.*, 2014, **136**, 14738–14741.

 This journal is © The Royal Society of Chemistry 2020

Published on 23 September 2020. Downloaded by University of Rochester on 10/20/2020 11:52:45 AM.

9 X. Yu, A. Mailman, K. Lekin, A. Assoud, C. M. Robertson, B. C. Noll, C. F. Campana, J. A. K. Howard, P. A. Dube and R. T. Oakley, *J. Am. Chem. Soc.*, 2012, **134**, 2264–2275.
10 A. Mailman, S. M. Winter, X. Yu, C. M. Robertson, W. Yong, J. S. Tse, R. A. Secco, Z. Liu, P. A. Dube, J. A. K. Howard and R. T. Oakley, *J. Am. Chem. Soc.*, 2012, **134**, 9886–9889.
11 D. Tian, S. M. Winter, A. Mailman, J. W. L. Wong, W. Yong, H. Yamaguchi, Y. Jia, J. S. Tse, S. Desgreniers, R. A. Secco, S. R. Julian, C. Jin, M. Mito, Y. Ohishi and R. T. Oakley, *J. Am. Chem. Soc.*, 2015, **137**, 14136–14148.
12 M. Souto, H. Cui, M. Peña-Álvarez, V. G. Baonza, H. O. Jeschke, M. Tomic, R. Valentí, D. Blasi, I. Ratera, C. Rovira and J. Veciana, *J. Am. Chem. Soc.*, 2016, **138**, 11517–11525.
13 N. Schiødt, T. Bjørnholm, K. Bechgaard, J. Neumeier and C. Allgeier, *Phys. Rev. B: Condens. Matter Mater. Phys.*, 1996, **53**, 1773–1778.
14 A. J. Schultz, H. H. Wang, H. W. Lynda, T. L. Sifter, J. M. Williams, K. Bechgaard and M. Whangbo, *Inorg. Chem.*, 1987, **26**, 3757–3761.
15 D. G. Branzea, F. Pop, P. Auban-Senzier, R. Clerac, P. Alemany, E. Canadell and N. Avarvari, *J. Am. Chem. Soc.*, 2016, **138**, 6838–6851.
16 N. Tenn, N. Bellec, O. Jeannin, L. Piekara-Sady, P. Auban-Senzier, J. Íñiguez, E. Canadell and D. Lorcy, *J. Am. Chem. Soc.*, 2009, **131**, 16961–16967.
17 G. Yzambart, N. Bellec, G. Nasser, O. Jeannin, T. Roisnel, M. Fourmigue, P. Auban-Senzier, I. Jorge, E. Canadell and D. Lorcy, *J. Am. Chem. Soc.*, 2012, **134**, 17138–17148.
18 E. Canadell, I. E.-I. Rachidi, S. Ravy, J. P. Pouget, L. Brossard and J. P. Legros, *J. Phys. France*, 1989, **50**, 2967–2981.
19 T. Isono, H. Kamo, A. Ueda, K. Takahashi, A. Nakao, R. Kumai, H. Nakao, K. Kobayashi, Y. Murakami and H. Mori, *Nat. Commun.*, 2013, **4**, 1–6.
20 Y. Kobayashi, T. Terauchi, S. Sumi and Y. Matsushita, *Nat. Mater.*, 2017, **16**, 109–114.
21 T. Jigami, K. Takimiya and T. Otsubo, *J. Org. Chem.*, 1998, **63**, 8865–8872.
22 D. Belo and M. Almeida, *Coord. Chem. Rev.*, 2010, **254**, 1479–1492.
23 M. M. Andrade, R. A. L. Silva, I. C. Santos, E. B. Lopes, S. Rabaça, L. C. J. Pereira, J. T. Coutinho, J. P. Telo, C. Rovira, M. Almeida and D. Belo, *Inorg. Chem. Front.*, 2017, **4**, 270–280.
24 A. Kobayashi, Y. Okano and H. Kobayashi, *J. Phys. Soc. Jpn.*, 2006, **75**, 051002.
25 T. Higashino, O. Jeannin, T. Kawamoto, D. Lorcy, T. Mori and M. Fourmigué, *Inorg. Chem.*, 2015, **54**, 9908–9913.
26 A. Filatre-Furcate, P. Auban-Senzier, M. Fourmigué, T. Roisnel, V. Dorcet and D. Lorcy, *Dalton Trans.*, 2015, **44**, 15683–15689.
27 H. Hachem, N. Bellec, M. Fourmigué and D. Lorcy, *Dalton Trans.*, 2020, **49**, 6056–6064.
28 J. Ren, W. Liang and M.-H. Whangbo, *Crystal and Electronic Structure Analysis Using CAESAR*, PrimeColor Software, Inc., Cary, NC, 1998.
29 R. Hoffmann, *J. Chem. Phys.*, 1963, **39**, 1397–1412.
30 M.-H. Whangbo and R. Hoffmann, *J. Am. Chem. Soc.*, 1978, **100**, 6093–6098.
31 M.-H. Whangbo, R. Hoffmann and R. B. Woodward, *Proc. R. Soc. London, Ser. A*, 1979, **366**, 23–46.
32 D. D. Perrin and W. L. F. Armarego, *Purification of Laboratory Chemicals*, Pergamon Press, Oxford, UK, 3rd edn, 1988.
33 *SMART and SAINT*, Bruker AXS Inc., Madison, WI, 2008.
34 G. M. Sheldrick, *SADABS*, Bruker AXS Inc., Madison, WI, 2004.
35 G. M. Sheldrick, *Acta Crystallogr., Sect. A: Found. Crystallogr.*, 2008, **64**, 112–122.
36 A. Altomare, M. C. Burla, M. Camalli, G. Cascarano, G. Giacovazzo, A. Guagliardi, A. G. G. Moliterni, G. Polidori and R. Spagna, *J. Appl. Crystallogr.*, 1999, **32**, 115–119.
37 G. M. Sheldrick, *Acta Crystallogr., Sect. C: Struct. Chem.*, 2015, **71**, 3–8.
38 L. J. Farrugia, *J. Appl. Crystallogr.*, 2012, **45**, 849–854.
39 C. F. Macrae, I. J. Bruno, J. A. Chisholm, P. R. Edgington, P. McCabe, E. Pidcock, L. Rodriguez-Monge, R. Taylor, J. van de Streek and P. A. Wood, *J. Appl. Crystallogr.*, 2008, **41**, 466–470.